

**Electronic supplementary information for High thermoelectric figure of merit in  
*p*-type Mg<sub>3</sub>Si<sub>2</sub>Te<sub>6</sub>: Role of multi-valley bands and high anharmonicity**

T. Pandey,<sup>1</sup> F. M. Peeters,<sup>1,2</sup> and M. V. Milošević<sup>1,3</sup>

<sup>1</sup>*Department of Physics, University of Antwerp, Groenenborgerlaan 171, B-2020 Antwerp, Belgium*

<sup>2</sup>*Departamento de Física, Universidade Federal do Ceará, Caixa Postal 6030, Fortaleza 60455-760, Brazil*

<sup>3</sup>*NANOLab Center of Excellence, University of Antwerp, Antwerp, Belgium*

(Dated: July 25, 2023)

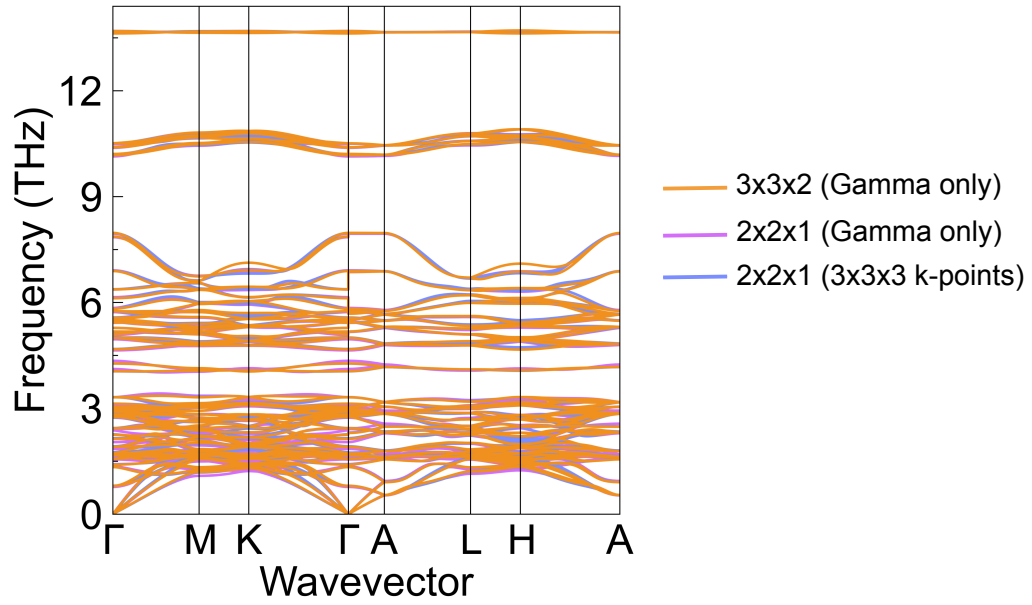


FIG. S1. Convergence of phonon dispersion with respect to the supercell size. Phonon frequencies are well converged on a  $2 \times 2 \times 1$  supercell.

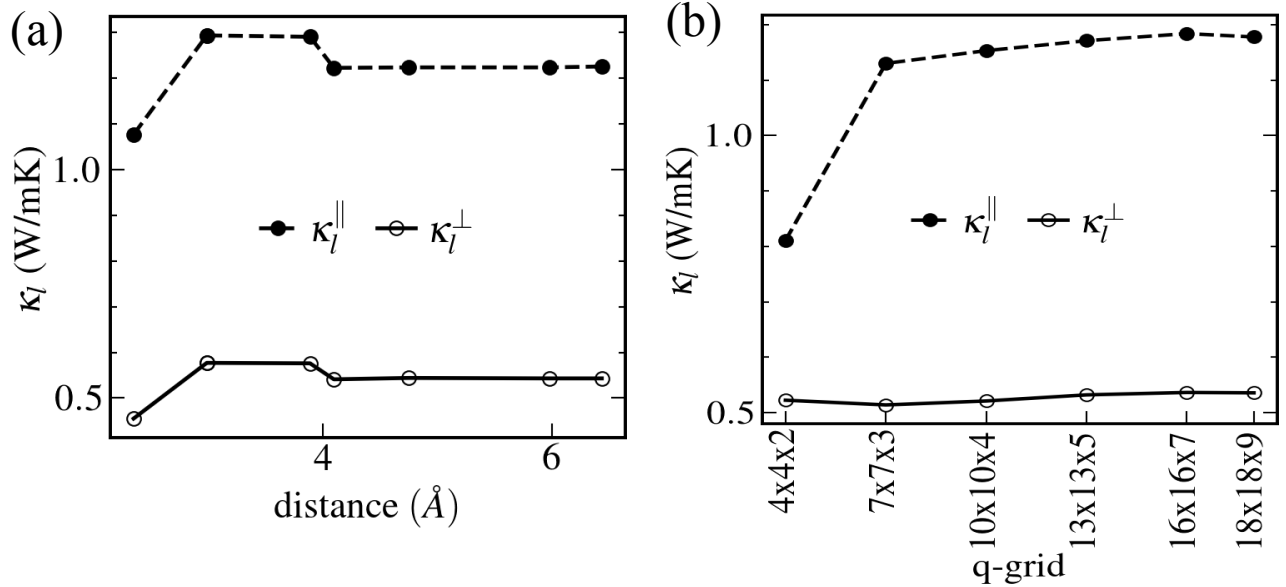


FIG. S2. Convergence of the room-temperature lattice thermal conductivity with respect to (a) nearest-neighbor cutoff used in 3rd order inter-atomic force constants, and (b) integration grid. Lattice thermal conductivity is well converged at interaction cutoff  $> 5$ , and integration grid of  $13 \times 13 \times 5$ .

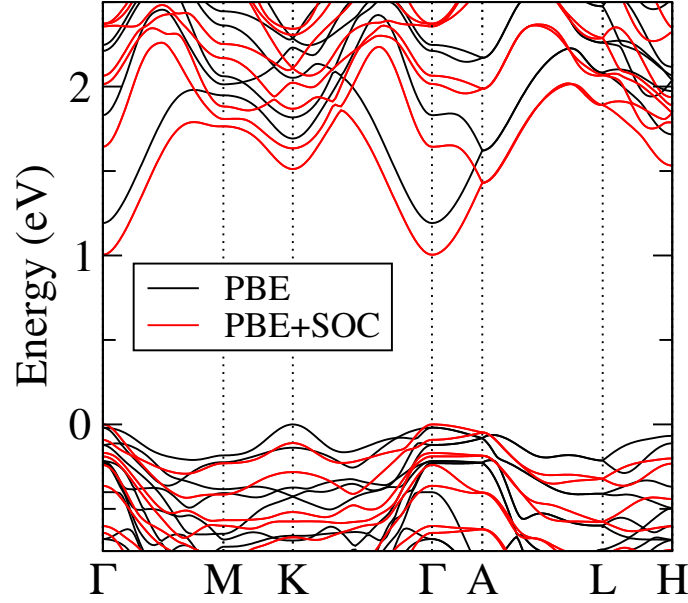


FIG. S3. Comparison of  $\text{Mg}_3\text{Si}_2\text{Te}_6$  band structure calculated without (PBE) and with spin-orbit coupling (PBE+SOC).

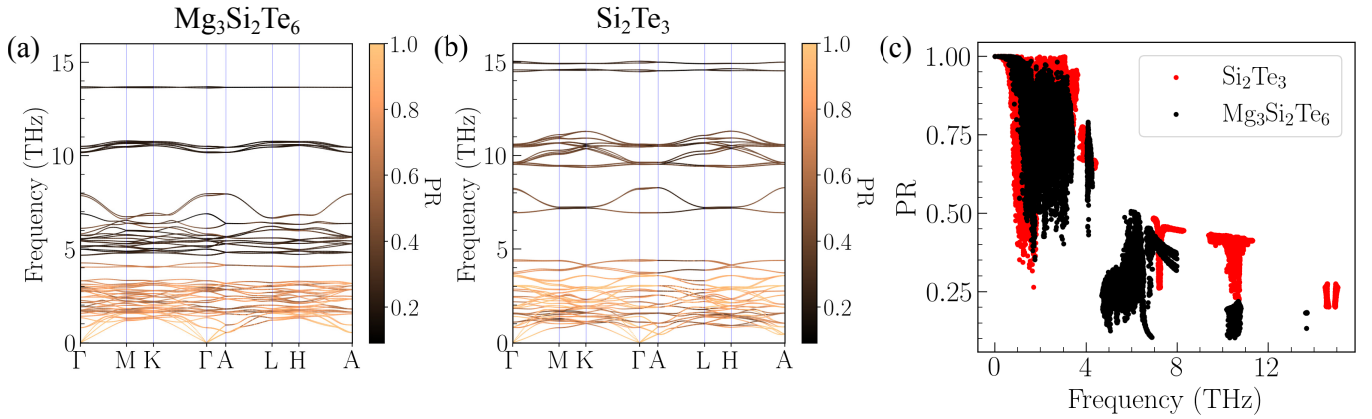


FIG. S4. Calculated participation ratio (PR) along the high symmetry path, in (a)  $\text{Mg}_3\text{Si}_2\text{Te}_6$  and (b)  $\text{Si}_2\text{Te}_3$ . (c) Comparison of PR in both compounds in the entire Brillouin zone. Lower PR value in  $\text{Mg}_3\text{Si}_2\text{Te}_6$  indicates that phonon modes in this compound are more localized. The most of localization is provided by Mg atoms.

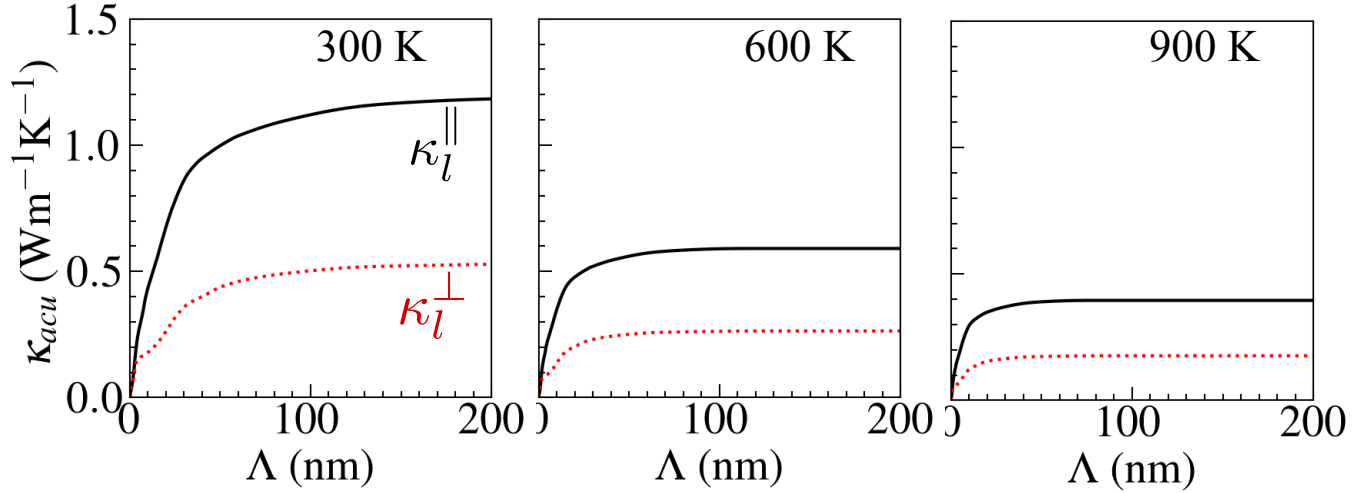


FIG. S5. Cumulative lattice thermal conductivity of  $\text{Mg}_3\text{Si}_2\text{Te}_6$  as a function of the mean free path at 300 K, 600 K, and 900 K. For mean free path in the range 10-20 nm,  $\kappa_l$  can be reduced by  $\sim 50\%$ .

TABLE S1.  $\text{Mg}_3\text{Si}_2\text{Te}_6$  parameters used for the electronic transport property calculations within AMSET code.  $\mathbf{C}$  is the elastic tensor in Voigt notation.  $\epsilon_s$  and  $\epsilon_\infty$  are the static and high-frequency dielectric constants, respectively.  $\omega_{PO}$  is the effective polar phonon frequency.

$\mathbf{C}$ (in GPa) =	$\begin{bmatrix} 68.14 & 19.39 & 11.57 & 0 & -2.0 & 0 \\ 19.39 & 68.14 & 11.57 & 0 & 2.0 & 0 \\ 11.57 & 11.57 & 39.20 & 0 & 0 & 0 \\ 0 & 0 & 0 & 13.58 & 0 & 2.0 \\ -2.0 & 2.0 & 0 & 0 & 13.58 & 0 \\ 0 & 0 & 0 & 2.0 & 0 & 24.33 \end{bmatrix}$
$\epsilon_s$ (in $\epsilon_0$ ) =	$\begin{bmatrix} 15.45 & 0 & 0 \\ 0 & 15.45 & 0 \\ 0 & 0 & 12.37 \end{bmatrix}$
$\epsilon_\infty$ (in $\epsilon_0$ ) =	$\begin{bmatrix} 9.95 & 0 & 0 \\ 0 & 9.95 & 0 \\ 0 & 0 & 7.26 \end{bmatrix}$
$\omega_{PO}$ (in THz) =	5.85

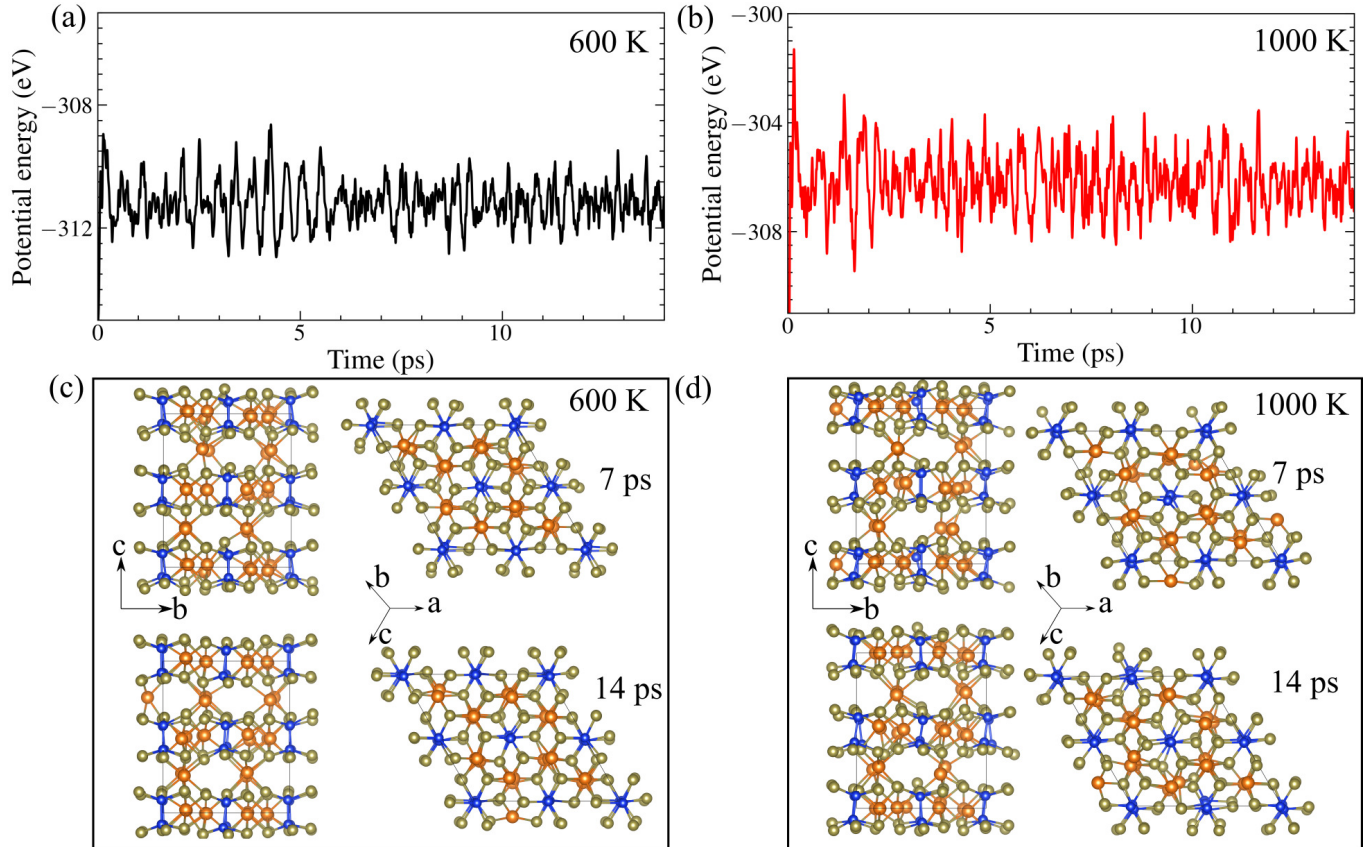


FIG. S6. (color online) Potential energy profiles of  $\text{Mg}_3\text{Si}_2\text{Te}_6$  during the AIMD simulation at (a) 600 K and (b) 1000 K, respectively. The corresponding 600 and 1000 K snapshots of atomic configurations at 7 and 14 ps are also shown in (c) and (d), respectively.